The Free Internet Journal for Organic Chemistry

Paper

Archive for Organic Chemistry

Arkivoc **2020**, part ii, 89-101

Infrared diagnostic of the conformational change of methylated β-glucose bound to Li^+ upon ligand addition

Oscar Alba Hernandez, Vincent Steinmetz, and Philippe Maître

Université Paris-Saclay, CNRS, UMR8000, Institut de Chimie Physique, 91405, Orsay, France
Email: philippe.maitre@universite-paris-saclay.fr

Dedicated to Professor José Manuel Riveros N. on the occasion of his 80th birthday and in recognition of his many seminal contributions to the gas phase physico chemistry of ions

Received 12-20-2019 **Accepted** 02-26-2020 **Published on line** 04-02-2020

Abstract

Infrared photodissociation spectroscopy in combination with tandem mass spectrometry (MS/MS) has been shown to provide diagnostic structural information on oligosaccharides. An investigation of the conformation of methylated β-glucose ionized with an alkali metal cation, and subsequently complexed by an ancillary ligand, is presented. On the basis of quantum chemical calculations, an interpretation of the variation of the IRMPD spectrum of the methylated β-glucose complexes is proposed. Two competing structural motifs are found to be at play, the energy ordering resulting from a subtle balance between the maximization of the coordination of the metal cation and intra-sugar hydrogen bonding.

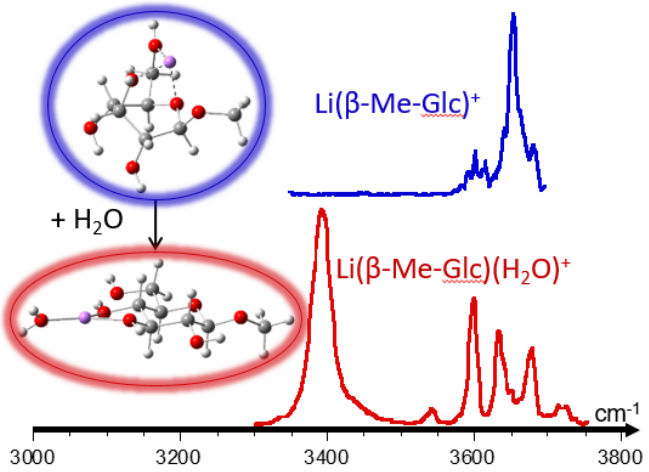

Keywords: Mass spectrometry, carbohydrates, isomers, differentiation, IR photodissociation, structural characterization

DOI: https://doi.org/10.24820/ark.5550190.p011.138

Introduction

Tandem mass spectrometry (MS/MS) is a method of choice for the analysis of oligosaccharides.[1] Separation and identification of these species is challenging because of the multiple sources of isomeric forms.[2] The structural diversity of natural and synthetic carbohydrates is associated with the inter-residue linkage positions and branching features. In addition, the anomeric configuration and stereochemistry of each monomer is another source of complexity. Fragmentation mass spectra of adducts of oligosaccharides and metal cations obtained using collision induced dissociation (CID) can be informative,[3] for the linkage types,[4,5] for example. As a result of this structural complexity, however, a comprehensive structural analysis is typically based on coupling of chromatographic separation techniques or, more recently, ion mobility spectrometry (IMS). IMS allows for the separation of glycans and structural information can be derived,[6] as was demonstrated in pioneering studies.[7-8] IMS-MS/MS instruments provide an added value since mobility-selected precursor ions can be reacted or dissociated, followed by mass analysis of the product ions.[9]

Improving the IMS separation and identification of IMS peaks associated with the different isomeric forms of saccharides is of current interest. Fragmentation mass spectra obtained upon photo-induced dissociation can be more informative than those obtained through CID.[10-14] Hence, using wavelength tunable laser sources, UV spectroscopy of mobility-selected disaccharides ions has emerged.[13-14] IR photo-dissociation spectroscopy of mobility-selected adducts of oligosaccharide and metal ions have also been performed more recently.[15-17] It should be noted, however, that these spectroscopic studies of large glycans were performed using a cryogenically cooled ion-trap. Well-resolved IR absorption features were derived allowing for an unambiguous structural diagnostic.[15] For instance, six disaccharide isomers that differ in their stereochemistry, attachment point of the glycosidic bond, and monosaccharide content were all unambiguously identified.[17] As demonstrated with a set of human milk oligosaccharides, the added dimension of IR spectroscopy allows for a fingerprint diagnostic of isomers of oligosaccharides ranging from trisaccharides to hexasaccharides, which could not be distinguished using IMS-MS/MS alone.[16] The recent development in traveling-wave IMS, called structures for lossless ion manipulation (SLIM),[18] offers an unprecedented mobility resolution. Using this ultrahigh SLIM resolution, it has been shown that glycan isomers that differ only in collisional cross section by 0.2 % can be separated and subsequently interrogated by IR spectroscopy in a cooled ion trap.[19-20] It should be stressed that the combination of IMS-MS/MS and IR spectroscopy allows for the separation and characterization of saccharides that differ by a single stereogenic center based on diagnostic features which can be typically found in the OH stretching region, where spectral shifts are directly related to the hydrogen bonding network.

In this paper we focus on the structure of methylated β-glucose coordinated to an alkali metal cation and on its conformational change induced upon addition of an ancillary ligand. The separation of methylated α-mannose, α-glucose, or β-glucose ionized with Li^+, Na^+, and K^+ was recently investigated by our group using differential mobility spectrometry (DMS). In the case of lithiated complexes, identification of the isomeric forms was achieved through infrared multiple photon dissociation (IRMPD) spectroscopy in the OH stretching region of the DMS-selected ions.[21] An IRMPD band near 3400 cm^{-1} was found to be highly structurally diagnostic. It was specifically observed for the two anomers of glucose, but not in the case of mannose. Herein, the conformation of methylated β-glucose in a complex formed with an alkali cation, and the conformational change induced upon the addition of an ancillary ligand, are probed using IRMPD spectroscopy. The conformational preference of the sugar unit is investigated using quantum chemical calculations, and computed IR absorption spectra of the low-lying isomers are used to analyze the conformational change of methylated β-glucose. Two competing structural motifs are found to be at play. The

energy ordering results from a subtle balance between maximization of coordination of the metal cation and the intrinsic conformational energetics of the saccharide, which is for a large part driven by hydrogen bonding.

Results and Discussion

Experimental IRMPD spectra of Li^+ complexes of methylated β-glucose. Experimental infrared spectra of alkali cation complexes of β-methylated glucose (β-Me-Glc) are given in Figure 1. The IRMPD spectra of Li(β-Me-Glc)$^+$ and monohydrated Li(β-Me-Glc)$(H_2O)^+$ complexes are given in panels a) and b), respectively. The IRMPD spectra of Li(β-Me-Glc)$(CH_3CN)^+$ and Na(β-Me-Glc)$(CH_3CN)^+$ complexes are given in panels c) and d). Expected bands in the 3000-3800 cm^{-1} spectral range for these complexes are associated with the CH and four OH stretches. The four OH stretches are the most structurally diagnostic. Free OH bands are expected near 3650-3700 cm^{-1}. When involved as hydrogen bond donors, however, the corresponding OH stretch band is red-shifted 83 and this red-shift is accompanied by a broadening.[22]

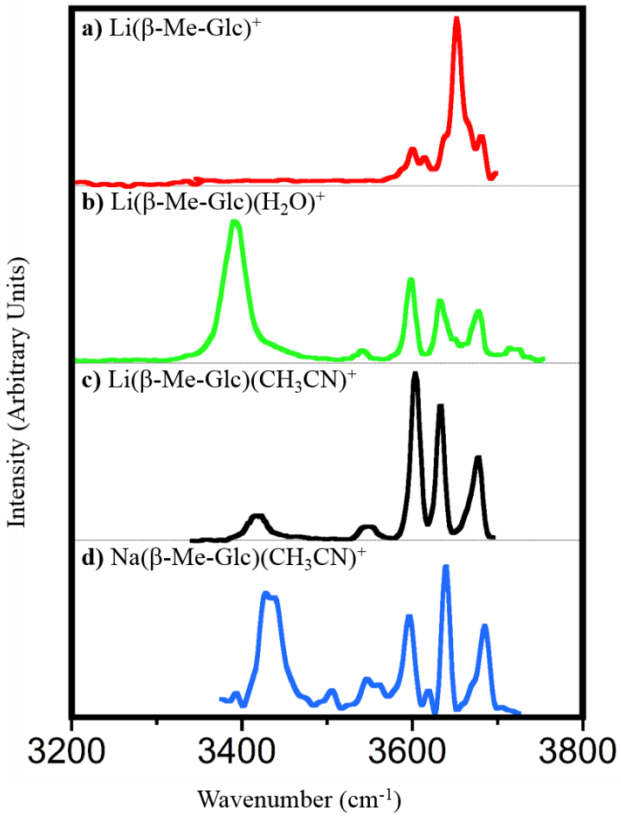

Figure 1. Experimental IRMPD spectra of a) Li(β-Me-Glc)$^+$ (red), b) Li(β-Me-Glc)$(H_2O)^+$ (green), c) Li(β-Me-Glc)$(CH_3CN)^+$ (black), and d) Na(β-Me-Glc)$(CH_3CN)^+$(blue) in the 3200-3800 cm^{-1} spectral range. The irradiation time was 1 s, and each OPO/OPA pulse was followed by a pulse of the auxiliary CO_2 laser. The CO_2 pulse duration was longer (5 ms) for the untagged Li(β-Me-Glc)$^+$ system, than for the tagged complexes (500 μs).

In the higher energy part of the spectra (3500-3800 cm^{-1}), bands corresponding to free or weakly hydrogen bonded OH stretches can be observed in the IR spectra of the Li(β-Me-Glc)$^+$ and monohydrated Li(β-Me-Glc)$(H_2O)^+$ complexes. In the latter case, bands associated with the two water OH stretches are expected

in addition to the four sugar OH stretches. In particular, the band observed near 3700 cm^{-1} for the Li(β-Me-Glc)$(H_2O)^+$ complex can be assigned to the asymmetric water OH stretch. Assignment of the other IR bands observed in the 3500-3800 cm^{-1} range for these two complexes is more difficult. Based on these high energy bands, it is difficult to draw conclusions regarding the conformation and/or interaction of the methylated β-glucose ligand with Li^+.

As stated above, these complexes are relatively strongly bound, and the auxiliary CO_2 laser had to be used to enhance their fragmentation. Since the OPO/OPA laser power drops when going from high to low frequency, two sets of OPO/OPA parameters were specifically optimized for recording the IRMPD spectra in the 3000-3500 and 3500-3800 cm^{-1}. CH stretching bands near 3000 cm^{-1} have been observed for the monohydrated Li(β-Me-Glc)$(H_2O)^+$ complex.[21] In the case of the Li(β-Me-Glc)$^+$ complex, however, no IRMPD band could be observed below 3500 cm^{-1}. This is likely due to the fact that the fragmentation threshold of the Li(β-Me-Glc)$^+$ complex is much larger than that of the corresponding monohydrated complex. As previously reported,[21] a band is observed near 3400 cm^{-1} for the monohydrated Li(β-Me-Glc)$(H_2O)^+$ complexes, which is a signature of a specific conformation of the sugar moiety. It thus seems that the addition of water to Li(β-Me-Glc)$^+$ may induce a conformational change of β-Me-Glc.

In order to probe the effect of the nature of alkali cation on the IR spectrum of methylated β-glucose complexes, sodium complexes were investigated since water binding to Na^+ is significantly lower than that to Li^+. Unfortunately, the Na^+ fragment formed upon IRMPD excitation of the Na(β-Me-Glc)$^+$ could not be detected with our MS/MS instrument. In addition, another consequence of Li to Na substitution is that no water adduct of Na(β-Me-Glc)$^+$ could be formed. Unfortunately, due to the instability of the Na(β-Me-Glc)$^+$ ion signal, the depletion spectrum is not reliable. We thus turn our attention to the addition of acetonitrile which is more strongly bound than water to Na^+. The IRMPD spectrum of the Na(β -Me-Glc)$(CH_3CN)^+$ complex is shown in Figure 1, along with the corresponding Li(β-Me-Glc)$(CH_3CN)^+$ spectrum. In both acetonitrile complexes, a broad band appears below 3500 cm^{-1}. The position of this broad band varies slightly from one complex to another. It is observed at ~3400, ~3420, and ~3430 cm^{-1} for the Li(β-Me-Glc)$(H_2O)^+$, Li(β-Me-Glc)$(CH_3CN)^+$, and Na(β-Me-Glc)$(CH_3CN)^+$ complexes.

To summarize, a band near 3350-3450 cm^{-1} was observed in all investigated complexes containing β-Me-Glc, except in the case of Li(β-Me-Glc)$^+$. Based on our previous study of monohydrated Li^+ complexes of methylated α-glucose, β-glucose, and α-mannose, it is concluded that a band near 3400 cm^{-1} is a clear structural diagnostic. Such a band was also observed for both Li(β-Me-Glc)$(H_2O)^+$ and Li(β-Me-Glc)$(H_2O)^+$ complexes.

One may wonder whether or not the low fragmentation efficiency of Li(β-Me-Glc)$^+$ prevents the observation of a band below 3500 cm^{-1} in a region where the OPO/OPA laser is relatively low. It is thus of interest to investigate the low energy structures of this complex, and to compare the corresponding IR absorption spectra to the IRMPD spectrum.

Low energy isomers of Li(β-Me-Glc)$^+$ complex. A representation of the 6-membered ring structure of a methylated hexose is given in Scheme 1. Four hydroxyl groups are available for hydrogen bonding, which is an important driving force for conformational stabilization. Due to the possible rotation about the C(5)-C(6) bond, the flexibility hydroxymethyl O(6)H group also plays an important role in deciding the structures of these systems. A hexose, in a pyranose form, can adopt different conformations including two chair forms ($^4C_1$ and $^1C_4$) or boat conformations.

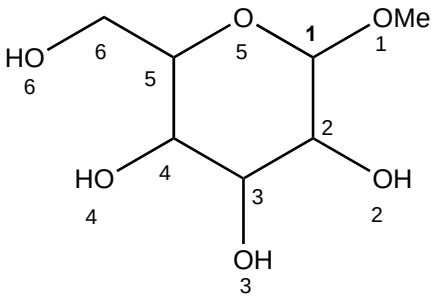

Scheme 1

The conformation of hexose derivatives has been studied theoretically.[23-26] In the case of the two glucose anomers, it has been established that the lowest energy structure has a $^4C_1$ chair configuration,[25] in both aqueous and gas phases. Different conformations of the $^4C_1$ chair have been characterized, and they essentially differ in the intramolecular hydrogen bonding network. The different conformers can thus be distinguished depending on the orientation of the hydroxyl groups and of the hydroxymethyl group.[27] The O(6)H group can interact, as a hydrogen bond donor or acceptor, with the O(4)H group, resulting in the formation of a six-membered hydrogen-bonded ring. The second type of conformer is characterized by a five-membered HB ring resulting from the HB interaction between the O(6)H donor and the ring O(5) oxygen atom. In the case of each glucose anomer, it was shown that the free energy at 298 K of the two types of conformers differ by less than 3 kJ/mol.[25]

In the present study, the starting point geometries for the structural search for the Li^+ complexes were the methylated sugar in a chair ($^4C_1$ or $^1C_4$) or boat conformation. For each conformation of the ring structure, different orientations of the OH groups were used as a starting point for geometry optimization. Particular care was taken with the hydroxymethyl group. The corresponding O(6)H hydroxyl can be involved in hydrogen bonding with equatorial O(4)H, or axial O(3)H hydroxyl groups, or O(5) intracyclic oxygen, depending on the hexose conformation ($^4C_1$ and $^1C_4$, respectively). The relative energies (kJ/mol) of the lowest energy structure associated with a chair ($^4C_1$ or $^1C_4$) and a boat configuration for the three methylated monosaccharides are given in Figure S1. 298K Gibbs free energies were calculated at the B3LYP/6-31G** level of theory.

As can be seen in Figure S1, the $^4C_1$ configuration is found to be the lowest in energy for the two methylated glucose anomers. A boat conformer is found to be lower than the lowest $^1C_4$ conformer. In the case of methylated β-glucose, the relative energies of the lowest energy boat and $^1C_4$ conformers are predicted to be 18.3 and 18.6 kJ mol^{-1}, respectively. This can be rationalized considering the number of intra-sugar hydrogen bonds. Only two hydrogen bonds can be formed when the methyl-β-glucose is in its $^1C_4$ chair conformation, while three hydrogen bonds can be formed in the case of the methyl-β-glucose in its $^1C_4$ chair conformation.

In the following, only the lowest energy structure associated with the adducts formed with Li^+ and sugar in a $^4C_1$, $^1C_4$, and boat are discussed. The lowest energy structures of each type of the sugar conformer ($^4C_1$, $^1C_4$, or boat) of Li(β-Me-Glc)$^+$ are given in Figure 2. The relative free energies at 298 K given in Figure 2 were determined at the B3LYP/6-31G** level of theory. Multiple isomers were considered for each conformation of the sugar unit, and the lowest energy isomers are shown in Figure S2.

If the methylated β-glucose is in $^4C_1$ chair conformation, it can only bind to the Li^+ cation as a bidentate ligand. Within all the corresponding optimized structures, the lowest energy one (β-Glc-C-34) is shown in Figure 2. The β-Glc-C-34 structure corresponds to the coordination of Li^+ to the O(3) and O(4) oxygen atoms. In addition, two O(4)H-O(6) and O(3)H-O(2) hydrogen bonds can be maintained. One can notice that the two

O(3)H and O(4)H hydroxyl groups which are bound to the Li^+ cation also acts as efficient HB donors. It is important to notice that the O(4)H-O(6)H distance is significantly shorter (1.81 Å) in the β-Glc-C-34 structure than in the low energy $^4C_1$ structures of free β-glucose, for which the typical bond distance is ~2 Å. This bond shortening upon binding to Li^+ is a signature of a synergic effect which has been observed for gas phase hydrated complexes of metal cations.[28] The hydrogen bond is reinforced when the hydrogen bond donor is coordinated to a metal cation.

It should be noted that the synergic effect is less pronounced if the O(3)H group is considered. The O(3)H-O(2) bond distance in β-Glc-C-34 and in the $^4C_1$ conformation of the free β-glucose are very similar. This difference in the Li^+ effect on the hydrogen bonding is probably due to the fact that the O(3)H-O(2) bond between two equatorial groups is relatively weak, while the O(4)H-O(6)H is much more favorable. In the latter case, the flexibility of the hydroxymethyl chain allows for the formation of a strong O(4)H-O(6)H hydrogen bond within a favorable six-membered ring motif.

This latter point might be at the origin of the preference for coordination through the O(4) and O(3) hydroxyl groups starting from the methylated β-glucose in its $^4C_1$ conformation. Other bidentate structures have been envisaged starting from a $^4C_1$ conformation, but they were found to be higher in energy. For example, the β-Glc-C-46 and β-Glc-C-23 structures are nearly degenerate, and are found to be about 10 kJ mol^{-1} higher in energy that the β-Glc-C-34 structure (See Figure S2).

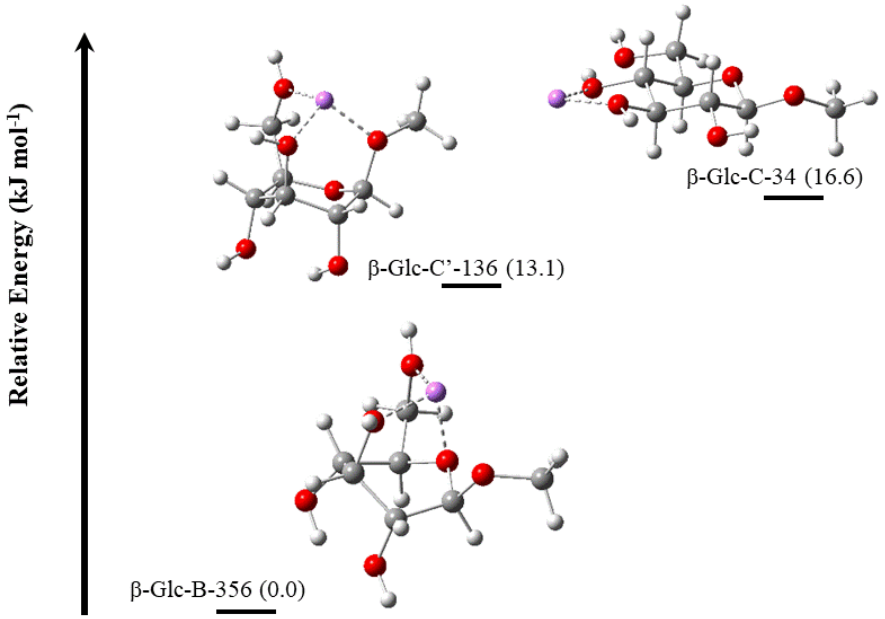

Figure 2. Relative free Gibbs energies of the most stable structures of the Li(β-Me-Glc)$^+$ complex. Three types of structures are considered, depending on the conformation of the sugar moiety: $^4C_1$, $^1C_4$ and boat conformers are denoted as C, C' and B, respectively. Only the most stable representative structure is shown here. Structures were characterized at the B3LYP/6-31G** level of theory. 298K Gibbs free energies are given in kJ mol^{-1}.

As can be seen in Figure 2, the β-Glc-C-34 structure of the Li(β-Me-Glc)$^+$ complex where the sugar unit acts as a bidentate ligand is not the lowest energy structure. In the case of the corresponding monohydrated Li(H_2O)(β-Me-Glc)$^+$ complex, this di-coordination mode of the sugar unit is preferred, and found in the lowest energy structure.[21]

The most energetically favored structure of Li(β-Me-Glc)$^+$ is the tri-coordinated β-Glc-B-356 derived from a boat conformer of the methylated β-glucose unit. This result may not be surprising since the lowest energy boat conformer of methylated β-glucose is only 18.3 kJ.mol^{-1} higher in energy than the $^4C_1$ chair, and that three oxygen atoms are available for Li^+ coordination in the former while only two are available in the latter leading to the β-Glc-B-356 and β-Glc-C-34, respectively. Furthermore, a close inspection of the Li^+-O distances reveals that this β-Glc-B-356 also has a relatively short Li^+-O(1) distance (2.5 Å), and it could thus be considered as a tetra-dentate structure. In addition, an intramolecular hydrogen bonding O(4)H-O(2) (2.04 Å) interaction can be preserved on the face of the sugar opposite to the Li^+ cation.

One structure (β-Glc-C'-136) derived from the sugar in its relatively low-energy $^1C_4$ conformation is predicted to be only 13.1 kJ mol^{-1} higher in energy than the β-Glc-B-356 structure. This tri-dentate structure probably also owes its relatively low energy to the hydrogen bond which is maintained between the O(2)H donor and the O(4) acceptor groups.

Structures of Na(α-glucose)$^+$ and Na(β-glucose)$^+$ with di-coordinated glucose in a chair conformation have been reported by Armentrout and coworkers.[29] The lowest energy structure of the Na(α-Glc)$^+$ was found to be a di-coordinated structure with the $^4C_1$ chair conformer acting as a bidentate ligand as in β-Glc-C-34 (Figure 2). Furthermore, the lowest energy structure of the Na(β-Glc)$^+$ system has the β-glucose in a boat conformation and acting as a tridentate ligand, very similar to the lowest energy β-Glc-B-356 structure found for Li(β-Me-Glc)$^+$. The lowest energy structures calculated by Armentrout and coworkers were consistent with the previous results obtained by Kentäma and coworkers for the arabinose and xylose systems,[26] with Barrows *et al.*[25] for the glucose systems, and Rahal-Sekkal *et al.*[30] for galactose saccharide. However, these results contrast with earlier results from Wesdemiotis and coworkers[31] on sodiated monosaccharide and disaccharide complexes.

Interpretation of the IRMPD spectra of Li(β-Me-Glc). Infrared spectra of Li(β-Me-Glc)$^+$ in the 3000-3800 cm^{-1} spectral range are shown of Figure 3. The experimental spectrum is given in the top panel. IR absorption spectra have been calculated for multiple types of coordination modes and hydrogen bonding. Only the calculated spectrum of the lowest energy structure of each type ($^4C_1$, $^1C_4$, boat) of the sugar conformation are given in the other panels of Figure 3. Calculated IR spectra of other low-lying isomers (see Figure S2) of Li(β-Me-Glc)$^+$ are given in Figure S3.

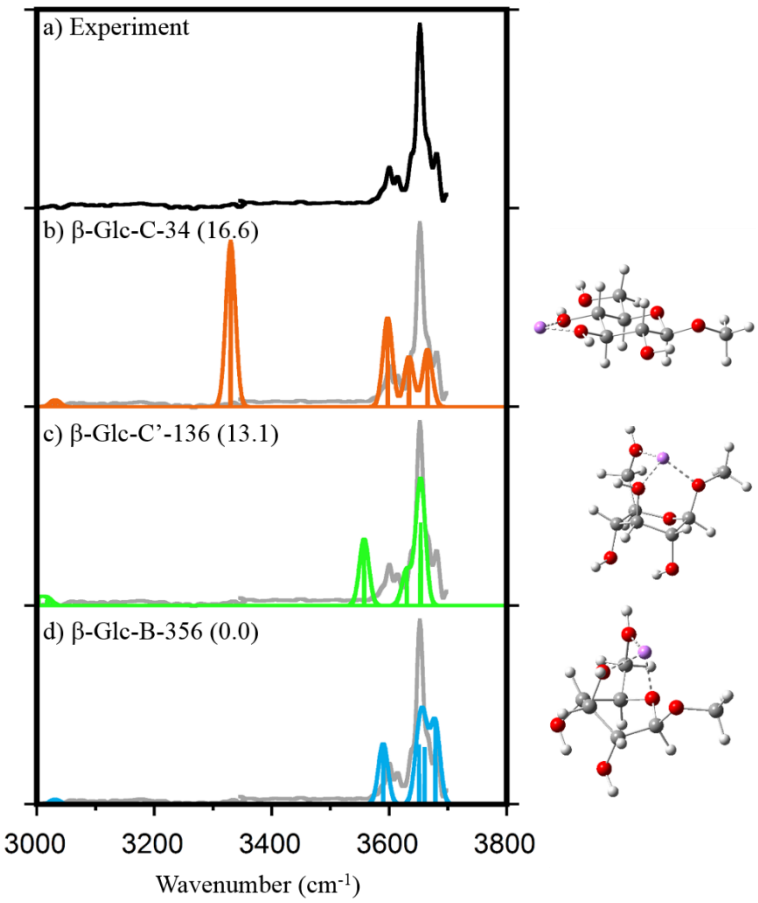

Figure 3. IRMPD spectrum of the Li(β-Me-Glc)$^+$ complex (upper panel). In the lower b-d panels the experimental IRMPD spectrum (grey) is compared to the most energetically favored structures with the methylated β-glucose in a $^4C_1$ chair (orange), $^1C_4$ chair (green), and boat (blue) conformation. The corresponding theoretical structures as well as the relative Gibbs free energies (in kJ mol^{-1}) are also provided. Theoretical infrared absorption spectra were calculated at the B3LYP/6-31G** level of theory, and each band was convoluted using a Gaussian profile with a fwhm of 20 cm^{-1}. Harmonic frequencies were scaled with a factor of 0.955.

The experimental spectrum has two broad and asymmetric features with a maximum at 3600 and 3660 cm^{-1}. The broad band at 3660 cm^{-1} has a shoulder on its blue side with a maximum at 3680 cm^{-1}, and also a less pronounced shoulder on its red side near 3640 cm^{-1}.

Within all the structures that have been characterized (Figure S2), the best match with the experimental IRMPD spectrum is found if the lowest energy structure (β-Glc-B-356) is considered. In this structure, the methylated β-glucose acts as a tridentate ligand and the three O(3), O(5), and O(6) oxygen atoms are bound to Li$^+$. A band assignment is proposed in Table 1 assuming that only the β-Glc-B-356 isomer is populated under our experimental conditions. The broad character of the band with a maximum at 3660 cm^{-1} is probably due to the fact that three IR absorption bands are predicted in this region for the β-Glc-B-356 isomer (Table 1). Three vibrational modes associated with nearly free OH stretches are predicted. Besides the band associated with the O(2)H stretching mode, which is predicted at 3660 cm^{-1}, the OH stretching modes of the O(3)H and O(6)H groups are predicted at 3652 and 3678 cm^{-1}, respectively. The last feature observed at ~3600 cm^{-1} can be assigned to the OH stretching mode of the O(4)H group which is predicted at 3589 cm^{-1}.

This band is slightly more red-shifted because it is involved as a donor in a hydrogen bond with the acceptor O(4)H group, and the corresponding intra-sugar hydrogen bond distance is 2.04 Å.

Table 1. Infrared band assignment of the Li(β-Me-Glc)$^+$ complex [a]

Vibrational Mode	Theory (cm^{-1})	Experiment (cm^{-1})
HB A O(6)H st	3678	
HB A O(2)H st	3660	3660
HB A O(3)H st	3652	
HB D O(4)H st	3589	3600

[a]Vibrational mode description is provided in the first column. Predicted scaled (by 0.955) harmonic frequencies and the experimental infrared band positions are given in columns 2, and 3, respectively.

As found for other molecular ions, the comparison of experimental IRMPD spectrum of the Li(β-Me-Glc)$^+$ complex against the calculated IR absorption spectra of the low energy isomers shows that a good match is observed if the lowest-energy structure is considered. As discussed in the context of IRMPD characterization of peptide fragments,[32] it is likely that thermalization of molecular ions through low energy collisions in the hexapole ion trap occurs. In some specific cases, kinetic trapping has been observed as in the case of the a_2 ion of a dipeptide which was formed in the hexapole linear ion-trap of the ICR.[33] Multiple low-energy isomers may be populated in some cases and thus contribute to the IRMPD spectrum.

In the present case, however, di-coordinated Li(β-Me-Glc)$^+$ structures such as β-Glc-C-34 can be discarded. This structure is characterized by a predicted IRMPD band near 3400 cm^{-1} which is not observed experimentally. This band is a highly structurally diagnostic and is associated with the O(4)H stretch which is simultaneously involved as a hydrogen bond donor and in the coordination of the alkali metal cation. As stated above, such a band is not observed for Li(β-Me-Glc)$^+$, but is observed upon addition of H_2O or CH_3CN, and is also observed in Na(β-Me-Glc)$(H_2O)^+$. As can be seen in Figure 1, the position of this band slightly varies from one system to the other. A blue shift observed from Li(β-Me-Glc)$(H_2O)^+$ to Li(β-Me-Glc)$(CH_3CN)^+$. This can be interpreted considering the gas phase basicity of the added ligand. The gas phase basicity of CH_3CN is higher (~370 kcal mol^{-1}) than that of H_2O (~30 kcal mol^{-1}). As a result, charge transfer to the Li^+ cation from the CH_3CN molecule is greater than that from the water molecule, which could explain the weakening of the Li--O(4)H bond, and consequently a blue-shift of the O(4)H frequency band from ~3400 to 3420 cm^{-1}.

Conclusions

The present study further confirms that wavelength tunable infrared multiple photon dissociation integrated to tandem mass spectrometry is a valuable tool for the identification of molecular ions. From an analytical point of view, this technique, orthogonal to MS/MS, provides a unique diagnostic fingerprint of mass-selected molecular ions.

Comparison of IRMPD spectra with IR absorption spectra derived from quantum chemical calculations on low-energy lying isomers allows for an unambiguous structural assignment. As found in many other examples, the best agreement is found when the lowest energy isomer is considered. Structural diagnostic can

also simply be based on the observation or not of the IR signature of a structural motif, which can be essential when there are multiple low-lying isomers.

In the present case, it was found that there are two competing structural motifs when methylated β-glucose is complexed with an alkali metal cation. IRMPD spectroscopy was found to provide a clear-cut diagnostic of conformational change of methylated β-glucose depending whether or not a second ligand was bound to the metal cation. The energy ordering of the two competing isomeric forms was found to be the result of a subtle balance between the maximization of the coordination of the metal cation and the intra-sugar hydrogen bonding.

Experimental Section

General. Infrared spectroscopy experiments were carried out using a 7 Tesla Fourier transform ion cyclotron resonance (FT-ICR) tandem mass spectrometer (Bruker Apex IV). This hybrid FT-ICR instrument is equipped with a so-called Qh interface featuring a quadrupole mass-filter and a linear hexapole ion-trap. Low-energy collisional thermalisation of the mass-selected ions can be achieved in this linear ion trap pressurized with Ar at ~10^{-3} mbar. If a trace amount of a molecule is seeded in argon, ion-molecule reactions can also be carried out in this ion trap.[34] In the present study, water and acetonitrile adducts of mass-selected ions were formed. Ions are then pulse-extracted into the ICR cell where they are mass-selected and subsequently irradiated with IR light. Details on the coupling of IR laser sources to this mass spectrometer can be found elsewhere.[34-35] An optical parametric oscillator/amplifier (OPO/OPA from LaserVision) laser system was used for recording the IR spectra in the 3000-3800 cm^{-1} region.[2] This laser system is pumped by an Innolas Spitlight 600 non-seeded Nd:YAG laser running at 25 Hz. The typical output energy of the OPO/OPA was 12–13 mJ/pulse at 3600 cm^{-1}. As proposed by Y.T. Lee,[36] an auxiliary CO_2 laser is used to enhance the fragmentation of strongly bound ions. Using our setup, ions are irradiated using a few ms long CO_2 pulse (10 watt continuous wave (CW), BFi OPTiLAS, France) following each OPO/OPA pulse, the delay being on the order of ~1 μs.[37-38] At 3600 cm^{-1} the typical bandwidth (fwhm) of the OPO/OPA laser system is 3–4cm^{-1}. Representative mass spectra recorded following IR irradiation of ICR mass-selected Li(β-Me-Glc)(CH3CN)+ and Li(β-Me-Glc)+ ions with the laser off- and off-resonance are given in Figure S4.

Sample solutions were prepared by mixing β-Me-Glc (Carbosynth) and alkali metal salts (Sigma-Aldrich) at a ratio of 1:20 in H_2O:CH_3OH=3:7 with a final concentration of 100 μM (saccharide) and 2 mM (metal salt). ESI conditions were as follow: Flow rate of 120 μL/h, desolvation gas flow of 5 L/min, nebulizer pressure of 10 psi, and desolvation gas temperature of 300 °C.

Quantum chemical calculations were performed for characterizing the isomeric structures of Li(β-Me-Glc)$^+$ and their corresponding IR absorption spectra. The Gaussian 09 package[39] was used throughout. An exhaustive characterization of the different conformers is out of the scope of this paper. We rather focused on the interpretation of the IRMPD spectrum of Li(β-Me-Glc)$^+$. The positions of the IR bands in the OH stretching region are very sensitive to the hydrogen bonding network and also to the coordination of the Li^+ by the different hydroxyl groups. Thus, starting from the low energy conformation of a chair ($^4C_1$ or $^1C_4$) or a boat conformation, the Li^+ cation was added. Different coordination sites were envisaged using various orientations of the hydroxyl and hydroxymethyl groups in order to find the best compromise between maximizing intra-sugar hydrogen bonding and Li^+ coordination.

The nomenclature used throughout this work for the structures can be illustrated using three examples: β-Glc-B-356, β-Glc-C'-136, and β-Glc-C-34. The numbers correspond to the number of the oxygen atoms bonded to the Li^+ cation. The $^4C_1$, $^1C_4$ or boat conformation is specified by a C, C', or B. Hence, structure β-Glc-B-356 corresponds to a boat β-Me-Glucose with O(3), O(5) and O(6) oxygen atoms bound to Li^+; structure β-Glc-C'-136 corresponds to a $^1C_4$ chair β-Me-Glucose with O(1), O(3) and O(6) oxygen atoms bound to Li^+; and structure β-Glc-C-34 corresponds to a $^4C_1$ chair β-Me-Glucose with O(3) and O(4) oxygen atoms bound to Li^+. Structures were optimized at the B3LYP/6-31G(d,p) level of theory. Gibbs free energies at 298K are considered for the relative energetics. IR absorption spectra were derived from harmonic calculations. A scaling factor of 0.955 was applied to the harmonic frequencies, as used previously to simulate the IR spectra in the X-H (X = O, N, C) stretching spectral range.[33-34]

Supplementary Material

Additional figures are pesented in the included supplementary material.

References

1. Kailemia, M. J.; Ruhaak, L. R.; Lebrilla, C. B.; Amster, I. J. *Anal. Chem.* **2014**, *86* (1), 196-212. https://doi.org/10.1021/ac403969n
2. Boltje, T. J.; Buskas, T.; Boons, G. J. *Nat. Chem.* **2009**, *1* (8), 611-622. https://doi.org/10.1038/nchem.399
3. Cancilla, M. T.; Penn, S. G.; Carroll, J. A.; Lebrilla, C. B. *J. Am. Chem. Soc.* **1996**, *118*, 6736-6745. https://doi.org/10.1021/ja9603766
4. Asam, M. R.; Glish, G. L. *J. Am. Soc. Mass Spectrom.* **1997**, *8*, 987-995. https://doi.org/10.1016/S1044-0305(97)00124-4
5. Hofmeister, G. E.; Zhou, Z.; Leary, J. A. *J. Am. Chem. Soc.* **1991**, *113*, 5964-5970. https://doi.org/10.1021/ja00016a007
6. Both, P.; Green, A. P.; Gray, C. J.; Sardzik, R.; Voglmeir, J.; Fontana, C.; Austeri, M.; Rejzek, M.; Richardson, D.; Field, R. A.; Widmalm, G.; Flitsch, S. L.; Eyers, C. E. *Nat. Chem.* **2014**, *6*, 65-74. https://doi.org/10.1038/nchem.1817
7. Liu, Y. S.; Clemmer, D. E. *Anal. Chem.* **1997**, *69*, 2504-2509. https://doi.org/10.1021/ac9701344
8. Lee, S.; Wyttenbach, T.; Bowers, M. T. *Int. J. Mass Spectrom.* **1997**, *167*, 605-614. https://doi.org/10.1016/S0168-1176(97)00105-5
9. Hilderbrand, A. E.; Myung, S.; Barnes, C. A. S.; Clemmer, D. E. *J. Am. Soc. Mass Spectrom.* **2003**, *14*, 1424-1436. https://doi.org/10.1016/j.jasms.2003.08.002
10. Vonderach, M.; Winghart, M. O.; MacAleese, L.; Chirot, F.; Antoine, R.; Dugourd, P.; Weis, P.; Hampe, O.; Kappes, M. M. *Phys. Chem. Chem. Phys.* **2014**, *16*, 3007-3013. https://doi.org/10.1039/c3cp54596b
11. Le, T. N.; Poully, J. C.; Lecomte, F.; Nieuwjaer, N.; Manil, B.; Desfrancois, C.; Chirot, F.; Lemoine, J.; Dugourd, P.; van der Rest, G.; Gregoire, G. *J. Am. Soc. Mass Spectrom.* **2013**, *24*, 1937-1949.

https://doi.org/10.1007/s13361-013-0722-x
12. Papadopoulos, G.; Svendsen, A.; Boyarkin, O. V.; Rizzo, T. R. *Faraday Discuss.* **2011**, *150*, 243-255. https://doi.org/10.1039/c0fd00004c
13. Lee, S.; Valentine, S. J.; Reilly, J. P.; Clemmer, D. E. *Int. J. Mass Spectrom.* **2012**, *309*, 161-167. https://doi.org/10.1016/j.ijms.2011.09.013
14. Zucker, S. M.; Lee, S.; Webber, N.; Valentine, S. J.; Reilly, J. P.; Clemmer, D. E. *J. Am. Soc. Mass Spectrom.* **2011**, *22*, 1477-1485. https://doi.org/10.1007/s13361-011-0179-8
15. Mucha, E.; Florez, A. I. G.; Marianski, M.; Thomas, D. A.; Hoffmann, W.; Struwe, W. B.; Hahm, H. S.; Gewinner, S.; Schollkopf, W.; Seeberger, P. H.; von Helden, G.; Pagel, K., *Ange. Chem. Int. Ed.* **2017**, *56*, 11248-11251. https://doi.org/10.1002/anie.201702896
16. Khanal, N.; Masellis, C.; Kamrath, M. Z.; Clemmer, D. E.; Rizzo, T. R. *Analyst* **2018**, *143*, 1846-1852. https://doi.org/10.1039/C8AN00230D
17. Masellis, C.; Khanal, N.; Kamrath, M. Z.; Clemmer, D. E.; Rizzo, T. R. *J. Am. Soc. Mass Spectrom.* **2017**, *28*, 2217-2222. https://doi.org/10.1007/s13361-017-1728-6
18. Deng, L. L.; Garimella, S. V. B.; Hamid, A. M.; Webb, I. K.; Attah, I. K.; Norheim, R. V.; Prost, S. A.; Zheng, X. Y.; Sandoval, J. A.; Baker, E. S.; Ibrahim, Y. M.; Smith, R. D. *Anal. Chem.* **2017**, *89*, 6432-6439. https://doi.org/10.1021/acs.analchem.7b00189
19. Ben Faleh, A.; Warnke, S.; Rizzo, T. R. *Anal. Chem.* **2019**, *91*, 4876-4882. https://doi.org/10.1021/acs.analchem.9b00659
20. Warnke, S.; Ben Faleh, A.; Scutelnic, V.; Rizzo, T. R. *J. Am. Soc. Mass Spectrom.* **2019**, *30*, 2204-2211. https://doi.org/10.1007/s13361-019-02333-0
21. Hernandez, O.; Isenberg, S.; Steinmetz, V.; Glish, G. L.; Maitre, P. *J. Phys. Chem. A* **2015**, *119*, 6057-6064. https://doi.org/10.1021/jp511975f
22. Walters, R. S.; Pillai, E. D.; Duncan, M. A. *J. Am. Chem. Soc.* **2005**, *127*, 16599-16610. https://doi.org/10.1021/ja0542587
23. Brown, J. W.; Wladkowski, B. D. *J. Am. Chem. Soc.* **1996**, *118*, 1190-1193. https://doi.org/10.1021/ja952804y
24. Jebber, K. A.; Zhang, K.; Cassady, C. J.; ChungPhillips, A. *J. Am. Chem. Soc.* **1996**, *118*, 10515-10524. https://doi.org/10.1021/ja960427z
25. Barrows, S. E.; Storer, J. W.; Cramer, C. J.; French, A. D.; Truhlar, D. G. *J. Comput. Chem.* **1998**, *19*, 1111-1129. https://doi.org/10.1002/(SICI)1096-987X(19980730)19:10<1111::AID-JCC1>3.0.CO;2-P
26. Guler, L. P.; Yu, Y. Q.; Kenttamaa, H. I. *J. Phys. Chem. A* **2002**, *106*, 6754-6764. https://doi.org/10.1021/jp025577c
27. Alonso, J. L.; Lozoya, M. A.; Pena, I.; Lopez, J. C.; Cabezas, C.; Mata, S.; Blanco, S. *Chem. Sci.* **2014**, *5*, 515-522. https://doi.org/10.1039/C3SC52559G
28. Walters, R. S.; Pillai, E. D.; Duncan, M. A. *J. Am. Chem. Soc.* **2005**, *127*, 16599-16610. https://doi.org/10.1021/ja0542587
29. Heaton, A. L.; Armentrout, P. B. *J. Phys. Chem. A* **2008**, *112*, 10156-10167. https://doi.org/10.1021/jp804113q

30. Rahal-Sekkal, M.; Sekkal, N.; Kleb, D. C.; Bleckmann, P. *J. Comput. Chem.* **2003**, *24*, 806-818. https://doi.org/10.1002/jcc.10223
31. Cerda, B. A.; Wesdemiotis, C. *Int. J. Mass Spectrom.* **1999**, *189*, 189-204. https://doi.org/10.1016/S1387-3806(99)00085-8
32. Hernandez, O.; Paizs, B.; Maitre, P. *Int. J. Mass Spectrom.* **2015**, *377*, 172-178. https://doi.org/10.1016/j.ijms.2014.08.008
Bythell, B. J.; Hernandez, O.; Steinmetz, V.; Paizs, B.; Maitre, P. *J. Mass Spectrom.* **2012**, *316*, 227-234. https://doi.org/10.1016/j.ijms.2012.02.020
33. Bakker, J. M.; Sinha, R. K.; Besson, T.; Brugnara, M.; Tosi, P.; Salpin, J. Y.; Maitre, P. *J. Phys. Chem. A* **2008**, *112*, 12393-12400. https://doi.org/10.1021/jp806396t
34. Bakker, J. M.; Besson, T.; Lemaire, J.; Scuderi, D.; Maitre, P. *J. Phys. Chem. A* **2007**, *111*, 13415-13424. https://doi.org/10.1021/jp074935e
35. Yeh, L. I.; Okumura, M.; Myers, J. D.; Price, J. M.; Lee, Y. T. *J. Chem. Phys.* **1989**, *91*, 7319-7330. https://doi.org/10.1063/1.457305
36. Sinha, R. K.; Erlekam, U.; Bythell, B. J.; Paizs, B.; Maitre, P. *J. Am. Soc. Mass Spectrom.* **2011**, *22*, 1645-1650. https://doi.org/10.1007/s13361-011-0173-1
37. Sinha, R. K.; Nicol, E.; Steinmetz, V.; Maitre, P. *J. Am. Soc. Mass Spectrom.* **2010**, *21*, 758-772. https://doi.org/10.1016/j.jasms.2010.02.014
38. Frisch, M. J.; Trucks, G. W.; Schlegel, H. B.; Scuseria, G. E.; Robb, M. A.; Cheeseman, J. R.; Scalmani, G.; Barone, V.; Mennucci, B.; Petersson, G. A.; Nakatsuji, H.; Caricato, M.; Li, X.; Hratchian, H. P.; Izmaylov, A. F.; Bloino, J.; Zheng, G.; Sonnenberg, J. L.; Hada, M.; Ehara, M.; Toyota, K.; Fukuda, R.; Hasegawa, J.; Ishida, M.; Nakajima, T.; Honda, Y.; Kitao, O.; Nakai, H.; Vreven, T.; Montgomery, J. A.; Peralta, J. E.; Ogliaro, F.; Bearpark, M.; Heyd, J. J.; Brothers, E.; Kudin, K. N.; Staroverov, V. N.; Kobayashi, R.; Normand, J.; Raghavachari, K.; Rendell, A.; Burant, J. C.; Iyengar, S. S.; Tomasi, J.; Cossi, M.; Rega, N.; Millam, J. M.; Klene, M.; Knox, J. E.; Cross, J. B.; Bakken, V.; Adamo, C.; Jaramillo, J.; Gomperts, R.; Stratmann, R. E.; Yazyev, O.; Austin, A. J.; Cammi, R.; Pomelli, C.; Ochterski, J. W.; Martin, R. L.; Morokuma, K.; Zakrzewski, V. G.; Voth, G. A.; Salvador, P.; Dannenberg, J. J.; Dapprich, S.; Daniels, A. D.; Farkas; Foresman, J. B.; Ortiz, J. V.; Cioslowski, J.; Fox, D. J., Gaussian 09, Revision B.01. **2009**.